Pseudouridinylation of mRNA coding sequences alters translation

Daniel E. Eyler[1,†], Monika K. Franco[2,†], Zahra Batool[3], Monica Z. Wu[4], Michelle L. Dubuke[5,6], Malgorzata Dobosz-Bartoszek[3], Joshua D. Jones[1], Yury Polikanov[3,7*], Bijoyita Roy[4*], and Kristin S. Koutmou[1,2*]

[1]University of Michigan, Department of Chemistry. [2]University of Michigan, Program in Chemical Biology. [3]University of Illinois, Chicago, Department of Biological Sciences, [4]New England Biolabs Inc., RNA and Genome Editing, Ipswich, MA, [5]University of Massachusetts, Proteomics and Mass Spectrometry Facility. [6]University of Massachusetts, Department of Biochemistry and Molecular Pharmacology. [7]University of Illinois at Chicago, Department of Medicinal Chemistry and Pharmacognosy

[†]Authors contributed equally. *Corresponding author.

This file includes:
Supplementary Materials and Methods;
Supplementary Discussion;
Supplementary Tables S1 to S7;
Supplementary Figures S1 to S18;
Supplementary References.

SUPPLEMENTAL MATERIALS AND METHODS

E. coli ribosomes.

Ribosomes were purified from *E. coli* MRE600. Cultures were inoculated with a 1:200 dilution of a saturated overnight culture and incubated with shaking at 37°C until an OD_{600} of 0.6. Cultures were transferred to an ice-water bath for 30 minutes before harvesting by centrifugation. Cell pellets were resuspended in Buffer A (20 mM Tris-Cl, 100 mM NH_4Cl, 10 mM $MgCl_2$, 0.5 mM disodium EDTA, 6 mM β-ME, pH 7.5) and lysed on a microfluidizer. The lysate was clarified by two subsequent centrifugations at 30,000×*g* for 15 minutes. Clarified lysate was layered onto 35 mL of Buffer D (20 mM Tris-Cl, 1.1 M sucrose, 500 mM NH_4Cl, 10 mM $MgCl_2$, 0.5 mM disodium EDTA, pH 7.5) and centrifuged for 18 hours at 4°C in a Beckman Type 45 Ti rotor. The centrifuge was set for minimal acceleration and deceleration rates. The supernatant was carefully removed, and the surface of the clear glassy pellets was rinsed with Buffer A. Pellets were resuspended in <5 mL of Buffer A by orbital shaking at 4°C. Tight-couple 70S particles were then isolated by rate-zonal ultracentrifugation in a Beckman Ti-15 zonal rotor through a 10-40% (w/v) sucrose gradient in Zonal Buffer (20 mM Tris-Cl, 60 mM NH_4Cl, 5.25 mM $MgCl_2$, 0.25 mM disodium EDTA, 3 mM β-ME, pH 7.5). A 50% (w/v) sucrose cushion in Zonal Buffer was used at the bottom of the rotor. After loading, the sample was centrifuged at 28,000 rpm for 19 hours at 4°C with no braking at the end of the run. A UA-6 absorbance detector with a high flow rate flow cell (Teledyne ISCO) was used to identify 70S-containing fractions. These fractions were pooled and ribosomes were concentrated by pelleting in the Type 45 Ti rotor. Pelleted 70S tight couples were resuspended in Buffer A, aliquoted, flash-frozen in liquid nitrogen, and stored at -80°C until use.

mRNAs and tRNAs for assays.

Unmodified mRNAs were prepared by run-off T7 transcription of DNA oligonucleotides (1). mRNAs containing modified nucleotides were synthesized and HPLC purified by Dharmacon. mRNA sequences were generally of the form GGUGUCUUGCGAGGAUAAGUGCAUU <u>AUG UUU UAA</u> GCCCUUCUGUAGCCA; the coding sequence is underlined. Purified *E. coli* transfer RNAs were purchased from MP Biomedical, Chemical Block, tRNA Probes (College Station, TX), or purified in our lab from bulk tRNA, and aminoacylated using S100 enzymes or partially purified synthetases (2). Bulk *E. coli* tRNA was purchased from Sigma.

Measurement of Ψ levels in purchased mRNA oligos by UHPLC-MS/MS

In the UHPLC-MS/MS assays RNA (200 ng) were first hydrolyzed to the composite mononucleosides via a two-step enzymatic hydrolysis using Nuclease P1 (500 U/µg RNA, overnight, pH 5.5, Thermo Fisher Scientific, Pittsburgh, PA) and recombinant shrimp alkaline phosphatase (2 U/µg RNA, four hours, pH 7.9, New England BioLabs, Ipswich, MA). The samples were lyophilized and reconstituted in 20 µL of water. LC-MS/MS analysis was performed using a Waters Acquity UPLC HSS T3 (100 x 2.1 mm, 1.8 µm, 100 Å) on a Vanquish ultrahigh-pressure liquid chromatograph (Thermo Fisher Scientific, Gemering, Germany) interfaced to a TSQ Quantum Ultra triple quadrupole mass spectrometer (Thermo Fisher Scientific, San Jose, CA). Mobile phase A was 0.01% (v/v) formic acid in water, and mobile phase B was 0.01% (v/v) formic acid in acetonitrile. The flowrate was 0.4 mL/min, and the gradient used was designed as previously published (3). The sample injection volume was 5 µL. The autosamples was kept at 4°C, and the column was held at 25°C in still air mode. Electrospray ionization was used in positive mode at 4.0 kV. The capillary temperature was 200°C, the vaporizer temperature was 350°C, the sheath gas was 10, and the auxiliary gas was 5. Ions were detected in tandem mass spectrometry (MS/MS) mode.

To quantify RNA nucleosides, calibration curves were created for the four main bases and four uridine modifications (pseudouridine, 5-methyluridine, 5-hydroxyuridine, and 2'-O-methyluridine). [^{13}C][^{15}N]-G (10 nM) was used as an internal standard. Automated peak integration was performed using XCalibur 3.0 MS software. All peaks were visually inspected to ensure proper integration (Figure S18). We observed peaks for only the four major bases and pseudouridine. Other modified bases were not present above background (<1% of total nucleosides). Comparison of the U:Ψ ratio in the oligos containing a UΨU codon suggests that there is a minority population (~20%) of "modified" oligos that contain U instead of Ψ. Since the effects of Ψ are relatively subtle (~2-fold), we are not able to distinguish the two populations in our ensemble experiments. Instead, the effect of the unmodified subpopulation is to shift the average behavior of the entire population towards the behavior of the unmodified mRNAs used as a control. As a consequence, our estimates of the effects of Ψ are under-estimates.

***E. coli* translation factors.**

Constructs for translation factors were from the laboratory of Dr. Rachel Green unless otherwise noted. IF-1 was expressed in BL21(DE3) at 17°C in Terrific broth overnight. Lysis, wash, and elution buffers contained 50 mM sodium phosphate, pH 7.8, 300 mM NaCl, 5 mM β-ME, and 10, 25, or 300 mM imidazole, respectively. IF-1 was purified by a single nickel-IMAC step and dialyzed overnight against storage buffer (100 mM Tris-Cl, 140 mM NH_4Cl, 60 mM KCl, 14 mM $MgCl_2$, 2

mM DTT), then diluted 2-fold with 50% glycerol and stored at −80°C. IF-2 was purified similarly, except that expression was at 37°C for 3 hours. IF-3 was expressed in LB media with 0.5 mM IPTG at 37°C for 3 hours. Lysis, wash, and elution buffers for nickel-IMAC were 20 mM Tris-Cl pH 7.5, 300 mM NaCl, 1 mM β-ME, with 5, 20, and 250 mM imidazole, respectively. Fractions containing IF-3 were pooled, concentrated, and dialyzed against storage buffer (50 mM Tris-Cl pH 7.5, 70 mM NH_4Cl, 7 mM $MgCl_2$, 1 mM DTT, 30 mM KCl, 20% glycerol (v/v)). EF-Tu was expressed in Terrific broth with 0.5 mM IPTG at 30°C overnight and purified by nickel-IMAC. Lysis buffer contained 20 mM Tris-Cl, 300 mM NaCl, 1 mM β-ME and 5 mM imidazole at pH 7.5. Wash buffer was 20 mM Tris-Cl, 500 mM NaCl, 1 mM β-ME, and 20 mM imidazole at pH 7.5. Elution buffer contained 20 mM Tris-Cl, 300 mM NaCl, 1 mM β-ME, and 250 mM imidazole at pH 8.5. Fractions containing EF-Tu were dialyzed against cleavage buffer (20 mM Tris-Cl, 200 mM NaCl, 2 mM β-ME) at 4°C overnight. TEV protease was added at a 1:100 mass ratio and incubated at 4°C overnight. TEV was removed by passage over a nickel-IMAC column. The unbound fraction was dialyzed against storage buffer (25 mM Tris-Cl, 75 mM NH_4Cl, 2.5 mM $MgCl_2$, 3 mM β-ME, 20 uM GDP, and 10% (v/v) glycerol) at 4°C overnight. EF-G was expressed and purified according to the same protocol as EF-Tu. Purified RF1 was a gift from Dr. Rachel Green. RF2 was purified from an RF2 overexpression strain (4) via three chromatographic steps: nickel-IMAC, Resource Q anion exchange, and Superdex 75 16/60 gel filtration. Lysis buffer was 30 mM Tris-Cl, 60 mM KCl, 5 mM β-ME at pH 7.5. IMAC-bound RF2 was washed with IMAC wash buffer A (30 mM Tris-Cl, 0.5 M KCl, 5 mM β-ME, pH 7.5), IMAC wash buffer B (30 mM Tris-Cl, 60 mM KCl, 10 mM imidazole, 5 mM β-ME, pH 7.5), and eluted with a gradient to 0.5 M imidazole in Wash Buffer B. Fractions containing RF2 were pooled, diluted with buffer IEX-A (30 mM Tris-Cl, 30 mM KCl, 5 mM β-ME, pH 7.5), and applied to a 6 mL Resource Q anion exchange column (GE Healthcare). Bound proteins were eluted with a linear gradient to buffer IEX-B (30 mM Tris-Cl, 1 M KCl, 5 mM β-ME, pH 7.5). Fractions containing RF2 were pooled, concentrated in centrifugal concentrators, and applied to a Superdex 75 16/60 gel filtration column equilibrated with storage buffer (30 mM Tris-Cl, 100 mM NH_4Cl, 30 mM KCl, 5 mM β-ME). RF2-containing fractions were pooled and glycerol was added to 25% (v/v). Purified RF2 was concentrated and stored at −80°C.

Formation of *E. coli* ribosome initiation complexes.

Initiation complexes (ICs) were prepared in 1X 219-Tris buffer (50 mM Tris pH 7.5, 70 mM NH_4Cl, 30 mM KCl, 7 mM $MgCl_2$, 5 mM β-ME) with 1 mM GTP. This buffer has been used extensively in the literature (5-7). Tight-couple 70S ribosomes (1 μM) were incubated with 1 μM mRNA, 2 μM each of IF-1, IF-2, and IF-3, and 1 μM f-[^{35}S]-Met-tRNA^{fMet} at 37°C for 30 minutes. Magnesium

chloride was added to a final concentration of 12 mM. Complexes were layered onto 1 mL of Buffer D (see "Ribosomes") in thick-wall polycarbonate tubes and centrifuged at 69,000 rpm in a Beckman TLA 100.3 rotor for 2 hours at 4°C. Pelleted complexes were resuspended in 1X 219-Tris buffer, flash-frozen in small aliquots and stored at −80°C.

In vitro amino acid addition assays.

Ternary complex was prepared by incubating EF-Tu with 10 mM GTP in 1X 219-Tris for 10 minutes at 37°C, then adding aminoacylated tRNA and incubating for another 15 minutes. Peptidyl transfer reactions contained 70 nM ICs and 1-2 μM ternary complex (1-2 μM aminoacylated tRNA, 20 μM EF-Tu, 5 mM GTP) in 1X 219-Tris buffer. Reaction aliquots were quenched with 500 mM KOH (final concentration) at discrete time points (0-600 seconds) either by hand or on a KinTek quench-flow apparatus. The reactants, intermediates and products at each time point were separated by electrophoretic TLC in pyridine-acetate buffer (20% acetic acid adjusted to pH 2.8 with pyridine) as previously described (6). Electrophoretic TLCs were visualized by phosophorimaging and quantified with ImageQuant. The data were fit using Equation 1:

$$Fraction\,product = A \cdot (1 - e^{k_{obs}t})$$

In vitro translation termination assays.

Pre-termination complexes were prepared on mRNAs containing the coding sequence AUG-UAA-GUU and AUG- ΨAA-GUU. Peptide release assays were performed in 1X219-Tris buffer at room temperature (100 nM pre-TCs, RF1/RF2 ranging from 50 nM to 10 μM). Reaction aliquots were quenched with 4% formic acid (final) at varying time points. Free f-[^{35}S]-Met was separated from f-[^{35}S]-Met-tRNA^{fMet} by electrophoretic TLC and quantified by phosphorimaging. For each timecourse the fraction of released ^{f}Met was fitted using Equation 1 to obtain an observed rate constant. $K_{1/2}$ values were obtained by fitting the k_{obs} vs. [RF] data points using Equation 2:

$$k_{obs} = k_{max} \cdot [RF]/(K_{1/2} + [RF])$$

In vitro assays with total aa-tRNA^{aa}

Initiation complexes and mRNA were generated as described above. Translation assays were performed by reacting IC complexes (70 nM final) with ternary complex (1 μM total tRNA aminoacylated with S100 enzymes or specific synthetases, 40 μM EF-Tu, 10 mM GTP) at room

temperature for 10 minutes. All assays were performed in 219-Tris buffer and quenched with 500 mM KOH (final concentration). Products were visualized by electrophoretic TLC, as described above.

EF-Tu single turnover GTP hydrolysis assays.

Partially purified *E. coli* initiator $tRNA_{fMet}$ (~3 nmol) was charged with [^{3}H]-methionine (specific activity 770 mCi/mmol) using purified synthetase and transformylase. After 30 minutes, the following components were added to the indicated final concentrations: 219-Tris buffer (1X), ribosomes (1.5 μM), mRNA (1.5 μM), IFs (3 μM), and GTP (1 mM). Incubation was continued for 30 minutes at 37°C, and initiation complexes were pelleted as described above. EF-Tu●phe-$tRNA_{phe}$●[^{32}P]-GTP ternary complex was prepared by incubating EF-Tu (~2 nmol, 40 μM) with [^{32}P]-GTP (50 μM, specific activity 47×10^{3} mCi/mmol) and EFTs (4.1 μM) for 15 minutes at 37 C. Purified phe-$tRNA_{phe}$ (~1 nmol) was added and incubation was continued for 10 minutes. Ternary complex was separated from free [^{32}P]-GTP on a ~3 mL G25 column in 1X219 buffer. Fractions containing the void volume peak were pooled, aliquoted, and snap frozen in liquid nitrogen. Aliquots of initiation complexes (~3 μM) and ternary complex (~600 nM) were thawed immediately before use and TC concentration was adjusted to ~200 nM with 1X219 buffer. Reactions were performed on a Kintek RQF-3 rapid quench using 10% formic acid as the quench solution. Timepoints were clarified by centrifugation and aliquots of each timepoint were separated on PEI-cellulose TLC plates in 0.5 M KPO_4, pH 3.5.

P site mis-match surveillance assays.

Procedure was adapted from Zaher and Green (6). Initiation complexes (ICs) were prepared on unmodified T7 transcripts (5'-GGUGUCUUGCGAGGAUAAGUGCAUUAUGUAAGUUGCCCUUCUGUAGCCA-3', see above) or synthetic mRNAs (Dharmacon; 5'-GGUGUCUUGCGAGGAUAAGUGCAUUAUGΨAAGUUGCCCUUCUGUAGCCA-3') in 1X 219-Tris buffer with 2 mM GTP. Initiation complexes were formed with 1 μM 70S *E. coli* ribosomes, 1 μM mRNA, 2 μM IF-1, IF-2, and IF-3, and 0.5 μM f-[^{35}S]-Met-$tRNA^{fMet}$ at 37°C for 30 minutes as described above. Ribosome Nascent Chain complexes (RNCs) were then formed by mixing equivalent volumes of initiation complexes and ternary complex containing EF-Tu (20 μM), Lys-$tRNA^{Lys}$ (4 μM), EF-G (10 μM), and GTP (5 mM) in 1X 219-Tris buffer and incubating at 37 °C for 15 minutes. Magnesium chloride was added to a final concentration of 12 mM and RNCs were then layered onto 1mL of Buffer D and then pelleted (please refer to **Formation of *E. coli***

ribosome initiation complexes above). P site mis-match surveillance assays were performed by mixing RNCs (70-100 nM final concentration) with RF2 (30mM) or a mixture containing both RF2 (30mM) and RF3 (30mM) in 2 mM GTP. The final magnesium concentration in these assays was 7mM. The reaction was quenched in 4% formic acid at discrete time points over a period of 10 minutes. Products were visualized by electrophoretic TLC, as described above.

In vitro assays for Val incorporation on UUU and YUU codons

Initiation complexes were prepared on mRNAs containing AUG-UUU-UAA or AUG-ΨUU-UAA mRNAs, pelleted, and resuspended at a concentration of 1 μM (see **Formation of E. coli ribosome initiation complexes**). Ternary complex was prepared in energy regeneration mix (1X Tris-219 buffer, 7 mM additional $MgCl_2$ for a total $MgCl_2$ concentration of 14 mM, 1 mM GTP, 3 mM phosphoenolpyruvate, 0.1 μg/mL pyruvate kinase) using 40 μM EFTu, 10 μM EFTs, and 10 μM Val-$tRNA_{Val}$. Reactions were performed in energy regeneration mix with 0.1 uM initiation complex and 10 μM Val-$tRNA_{Val}$•EFTu•GTP ternary complex. Aliquots were withdrawn at timepoints and quenched with an equal volume of 1 M KOH. After quenching samples were neutralized with acetic acid, and peptide products were separated by electrophoretic TLC (pyridine-acetate buffer, pH 2.8, 1200V, 35 minutes) and quantified by phosphorimaging.

Crystallographic structure determination.

Ribosome complex containing mRNA and tRNAs was pre-formed by mixing 5 μM 70S Tth ribosomes with 10 μM Ψ-mRNA and incubation at 55°C for 10 minutes, followed by addition of 20 μM P site ($tRNA_i^{Met}$) and 20 μM A site ($tRNA^{Phe}$) substrates (with minor changes from (8)). At each of these two steps ribosome complexes were incubated for 10 minutes at 37°C in the buffer containing 5 mM HEPES-KOH (pH 7.6), 50 mM KCl, 10 mM NH_4Cl, and 10 mM $Mg(CH_3COO)_2$. Crystals were grown by vapor diffusion in sitting drop crystallization trays at 19°C. Initial crystalline needles were obtained by screening around previously published ribosome crystallization conditions (9-11). The best-diffracting crystals were obtained by mixing 2-3 μL of the ribosome-mRNA-tRNA complex with 3-4 μL of a reservoir solution containing 100 mM Tris-HCl (pH 7.6), 2.9% (w/v) PEG-20K, 7-12% (v/v) MPD, 100-200 mM arginine, 0.5 mM β-mercaptoethanol (8). Crystals appeared within 3-4 days and grew up to 200 × 200 × 1000 μm in size within 10-12 days. Crystals were cryo-protected stepwise using a series of buffers with increasing concentrations of MPD until reaching the final concentration of 40% (v/v) MPD, in which they were incubated overnight at 19°C. In addition to MPD, all stabilization buffers contained 100 mM Tris-HCl (pH 7.6), 2.9% (w/v) PEG-20K, 50 mM KCl, 10 mM NH_4Cl, 10 mM $Mg(CH_3COO)_2$ and 6 mM β-

mercaptoethanol. After stabilization, crystals were harvested and flash frozen in a nitrogen cryo-stream at 80K.

Diffraction data were collected on the beamlines 24ID-C and 24ID-E at the Advanced Photon Source (Argonne National Laboratory, Argonne, IL). A complete dataset for each ribosome complex was collected using 0.979Å wavelength at 100K from multiple regions of the same crystal using 0.3° oscillations. The raw data were integrated and scaled using the XDS software package (12). All crystals belonged to the primitive orthorhombic space group $P2_12_12_1$ with approximate unit cell dimensions of 210Å x 450Å x 620Å and contained two copies of the 70S ribosome per asymmetric unit. Each structure was solved by molecular replacement using PHASER from the CCP4 program suite (13). The search model was generated from the previously published structure of the *T. thermophilus* 70S ribosome with bound mRNA and tRNAs (PDB entry 4Y4P from (8)). The initial molecular replacement solutions were refined by rigid body refinement with the ribosome split into multiple domains, followed by ten cycles of positional and individual B-factor refinement using PHENIX (14). Non-crystallographic symmetry restraints were applied to 4 domains of the 30S ribosomal subunit (head, body, spur, helix 44), and 4 domains of the 50S subunit (body, L1-stalk, L10-stalk, C-terminus of the L9 protein).

The final model of the 70S ribosome in complex with mRNA/tRNAs was generated by multiple rounds of model building/fitting in COOT (15), followed by refinement in PHENIX (14). The statistics of data collection and refinement are compiled in Table S2. All figures showing atomic models were generated using PyMol software (www.pymol.org).

After we first observed no density for the CCA-end of the A-site tRNA, we repeated this experiment multiple times and collected about a dozen of datasets. The dataset reported here was collected from a single crystal. This dataset has the best resolution and overall best quality out of all collected datasets. Basically, there is a complete absence of any presence of the CCA end. In all our control datasets, in which we've used the same batch of $tRNA^{Phe}$ and regular unmodified mRNA, the CCA tail was clearly visible in the electron density and formed canonical WC interactions with the A loop of the 23S rRNA:Phe tRNA. The quality of the electron density and the resolution of the ΨUU containing structure in the vicinity of the PTC is not any worse than any of the datasets that we used as controls, which all have the same overall resolution. Specifically, the electron density is clearly visible for all of the key nucleotides in the PTC, such as 2451, as well as the nucleotides forming the A and P loops. Moreover, the P-loop interactions of the P-site tRNA are clearly visible in the P site.

Plasmid construction for in vitro transcription of luciferase mRNA for *in vivo* expression.

The template for in vitro synthesis of luciferase mRNA comprise, from 5′ to 3′: the T7 promoter, followed by an N-terminal 3× Hemagglutinin (HA) tag fused in-frame with the firefly luciferase gene, in-frame C-terminal StrepII and FLAG tags. The open reading frame spans from the 3xHA tag to the FLAG tag enabling the purification of full-length luciferase protein and not translation truncated products. The beta-globin 5' and 3' untranslated region (UTR) sequences were used for the expression of luciferase mRNA. Plasmids were generated by PCR and standard molecular cloning techniques.

In vitro transcription of luciferase mRNA.

mRNA was transcribed using T7 RNA polymerase (New England Biolabs) from a linearized plasmid or PCR-amplified linear template. All four nucleoside triphosphates in the reaction, natural or modified, were used at a final concentration of 4 mM. For generation of nucleoside-modified mRNAs, UTP was replaced with triphosphate-derivative of pseudouridine (Trilink). The in vitro transcribed RNAs were treated with Turbo DNaseI (Invitrogen) and followed by spin column clean-up (New England Biolabs). The mRNAs were post-transcriptionally capped with Vaccinia capping enzyme and treated with Cap 2'-O Methyl Transferase (New England Biolabs) to increase the stability and the translation efficiency of the luciferase mRNA.

mRNA transfection and expression analyses.

Synthesized, purified mRNAs were transfected into 293H cells using TransIT-mRNA transfection kit as recommended by the manufacturer (Mirus). The expression of the luciferase mRNA was analyzed by western blot analyses at various time points (15, 30, 60, 90, 120, 180, 240, 300, 360 minutes post-transfection) and cells were harvested 6-hours post transfection. Tandem purification of the luciferase translation products was performed using the FLAG tag followed by selection for the N-terminal HA tag as described previously (16, 17). The purified products were analyzed on 8% SDS-PAGE, gels were then silver stained (ProteoSilver, Sigma) and processed for mass spectrometry. Three independent transfections were performed for uridine/Ψ -containing mRNAs. For western blot analyses of the luciferase protein, proteins were separated by SDS-PAGE and blotted to 0.45 μm PVDF membranes (GE Healthcare). The blots were probed with an anti-HA antibody (Sigma). IR Dye™ -680 and -800 conjugated secondary conjugated antibodies were from Cell Signaling Technologies.

In-gel Digestion and LC-MS/MS Analysis.

Silver-stained gel bands containing the luciferase protein were de-stained in 1 mL of 15 mM potassium ferricyanide and 50 mM sodium thiosulfate, with gentle shaking, for 30 minutes. The gel band was then subjected to in-gel trypsin digestion after reduction with dithiothreitol and alkylation with iodoacetamide. Peptides eluted from the gel were lyophilized and re-suspended in 25µL of 5% acetonitrile (0.1% (v/v) TFA). A 3 µL injection was loaded by a Waters NanoAcquity UPLC in 5% acetonitrile (0.1% formic acid) at 4.0 µL/min for 4.0 min onto a 100 µm I.D. fused-silica pre-column packed with 2 cm of 5 µm (200Å) Magic C18AQ (Bruker-Michrom). Peptides were eluted at 300 nL/min from a 75 µm I.D. gravity-pulled analytical column packed with 25 cm of 3 µm (100Å) Magic C18AQ particles using a linear gradient from 5-35% of mobile phase B (acetonitrile + 0.1% formic acid) in mobile phase A (water + 0.1% formic acid) over 45 minutes. Ions were introduced by positive electrospray ionization via liquid junction at 1.4kV into a Thermo Scientific Q Exactive hybrid mass spectrometer. Mass spectra were acquired over *m/z* 300-1750 at 70,000 resolution (*m/z* 200) with an AGC target of 1e6, and data-dependent acquisition selected the top 10 most abundant precursor ions for tandem mass spectrometry by HCD fragmentation using an isolation width of 1.6 Da, max fill time of 110 ms, and AGC target of 1e5. Peptides were fragmented by a normalized collisional energy of 27, and fragment spectra acquired at a resolution of 17,500 (*m/z* 200).

Data Analysis – Identification of amino acid substitutions.

Raw data files were peak-picked by Proteome Discoverer (version 2.1), and preliminary searches were performed using the MASCOT search engine (version 2.4) against the *SwissProt Human* FASTA file (downloaded 05/2018) modified to include the luciferase protein sequence. Search parameters included Trypsin/P specificity, up to 2 missed cleavages, a fixed modification of carbamidomethyl cysteine, and variable modifications of oxidized methionine, pyroglutamic acid for Q, and N-terminal acetylation. The processed peak list was then re-searched in MASCOT against luciferase only, using an error-tolerant search allowing for all amino acid substitutions. High probability substitutions, as determined by greater than 90% peptide probability in Scaffold (version 4.8.8), were then added back to the original search parameters in Proteome Discoverer for interrogation by MASCOT as variable modifications for confirmation.

Data Analysis – Quantitation of amino acid substitutions.

The final search, with confirmed variable modifications, was loaded into Skyline-daily (University of Washington, version 4.1) as a spectral library. Each raw file was loaded, generating an

extracted ion chromatogram for each peptide of interest, and each peak was manually inspected for proper peak picking, isotope dot product ≥ 0.8, good fragment ion coverage, and elution times in line with the time of MS/MS identification of the peptide. The sum of the top 3 isotopes were then exported for each modification for further analysis.

In vitro translation of luciferase mRNA

Luciferase mRNAs transcribed either with 100% uridine or 100% pseudouridine (see In vitro transcription of luciferase mRNAs) were translated in vitro using PURExpress® (New England Biolabs). Each reaction contained 60-100 pmol luciferase mRNA and 50-76 µCi of L-[35S]-Methionine (Perkin Elmer), and PURExpress® (NEB) kit components according to manufacturer instructions. Reactions were incubated at 37 °C and aliquots removed at various time points (0, 2, 10, 30, 60, 120, 180, 240 mins). Samples were quenched with 1X SDS loading buffer (final concentrations 0.25mM Tris-HCl pH 6.8,12.5% Glycerol, 0.5% Bromophenol blue, 5% SDS, 50 mM β-mercatoethanol), and placed on ice. Samples were heated at 95 °C for five minutes and then loaded on a 4–12% Criterion™ XT Bis-Tris Protein Gel (BioRad) and electrophoresed at 90 V for 3 hours in 1X XT MOPS buffer (BioRad). The gel was then fixed in a solution of methanol/acetic acid/water (45%/10%/45% v/v/v) for 5 minutes at room temperature. The gels were then dried on filter paper at 80 °C for one hour. Gels were visualized by phosophorimaging and quantified with ImageQuant.

SUPPLEMENTAL DISCUSSION

Effects of modified bases on peptide release at stop codons

We investigated how Ψ impacts translation of nonsense codons. Ψ in stop-codons has been shown to promote translational read-through of stop-codons in both bacteria (18) and eukaryotes (19) and alter the conformation of the critical ribosomal RNA bases A1492 and A1493 in ribosomes crystallized with A site mismatches (18). Theoretical studies predicted that Ψ might perturb peptide release due to a difference in dipole moment, where pseudouridinylated stop codons have a ~30% smaller angular difference, leading to weaker helical interactions and weaker interactions with RF1 (20). However, the only in vitro study to date with ribosomes terminating on Ψ containing stop-codons found no difference between RF1-catalyzed release on modified and un-modified codons (21). We performed a similar set of studies under different buffer conditions and find that the action of RF1, but not RF2, is impacted by the presence of Ψ (Figure 4). Our RF2 results are not comparable to the previous study since the previous study used the A246T variant of RF2 with decreased activity (4, 22). Although there is a small discrepancy between our RF1 result and the published report (21) is puzzling, our results generally support this finding, and do not suggest that Ψ is likely to dramatically suppress translation termination in in vivo under normal cellular conditions (6, 23-27). More detailed structural and mechanistic investigation of tRNA selection and RF1-mediated peptide release on Ψ-containing codons will therefore be rewarding.

Our data suggest that the affinity of RF2 for UAm^{6}A codons may be reduced. An earlier study demonstrated that RF2, but not RF1, inefficiently terminates translation on a full-length ErmCL reporter when an O6 carbonyl group is substituted for an N6 amino group in an adenosine present at the third position of a stop-codon (28). While m^{6}A does not have an O6 group, the additional methyl group similarly removes the ability of the adenosine to form hydrogen-bonds at N6, and also increases the steric bulk nucleobase. Our findings support the idea that the presence of an N6 amino group at A3 is important for RF2 catalyzed peptide release on stop codons (28).

Important considerations in mass spectrometry analysis of peptides with alternative decoding

The detection of amino-acid substituted peptides by mass spectrometry is difficult due to the low frequency of the initial event and the fact that the signal is distributed amongst the several different possible substitutions. Careful design of the assay system was therefore required to permit detection of amino acid substituted peptides. For these studies, luciferase mRNA was transcribed in vitro with either uridine or Ψ and transfected into 293H cells and their expression

was comparable (Fig. S4). We performed tandem purification of the luciferase protein with N-terminal HA and C-terminal FLAG tags to eliminate analyses of premature translation truncation products. Equal amounts of luciferase protein expressed from uridine- and Ψ-containing mRNAs were subjected to mass spectrometric analyses (Fig. S5). To ensure detection of low frequency events the codons were first analyzed on a specific luciferase peptide (^{41}KGPAPFYPLEDGTAGEQLHK^{60}) that is highly represented in the spectra (16, 17). An error-tolerant search allowing for identification of any of the 20 possible amino acids substituted at a specific position in the peptide was performed. To analyze if Ψ promoted amino acid substitution in cells, we assessed if substitution events took place at several U-containing codons (Fig. 4C, Table S4). For the peptide of interest, no amino acid substitutions were detected on the samples generated from uridine-containing mRNAs, while the peptide generated from Ψ-containing mRNAs contained several low-frequency amino acid substitutions (totaling ~1%) (Fig. S6, Table S5). We also extended our analyses to the entire luciferase dataset. Luciferase protein translated from Ψ-containing mRNAs possessed a significantly higher rate of amino acid substitution (totaling ~1.5%, integrated over all U-containing codons) relative to protein synthesized from uridine-containing mRNAs (substitutions only on two < 0.05% Val codons were observed) (Table S6).

SUPPLEMENTARY TABLES

Table S1.

Single turnover rate constants for amino acid addition and GTP hydrolysis. This table reflects the values plotted in Figure 1C for the ribosome catalyzing the addition of a single phenylalanine on unmodified and modified codons, and the values shown in Figure 2B for GTP hydrolysis by the EF-Tu●phe-tRNA$_{phe}$●[^{32}P]-GTP ternary complex. The reported k_{obs} and standard error values are from the fit of a single curve to all replicate time courses. N.D., not determined.

Codon	k_{obs} (s^{-1}) ± SE	Maximum % ^{f}Met in MF (endpoint)	k_{GTP} (s^{-1}) ± SE
UUU	5.1 ± 0.4	71 ± 6	78.5 ± 9.5
ΨUU	2.1 ± 0.3	68.7 ± 3.8	42.2 ± 6.1
UΨU	2.9 ± 0.2	63.5 ± 1	N.D.
UUΨ	2.3 ± 0.2	72 ± 3	N.D.

Table S2. X-ray data collection and refinement statistics.

Crystals		70S complex with ΨUU-mRNA and A-, P- and E-tRNAs
Diffraction data		
Space Group		$P2_12_12_1$
Unit Cell Dimensions, Å (a x b x c)		208.73 x 445.1 x 613.63
Wavelength, Å		0.9795
Resolution range (outer shell), Å		360-2.95 (3.03-2.95)
I/σI (outer shell with I/σI=1)		4.95 (0.89)
Resolution at which I/σI=1, Å		2.95
Resolution at which I/σI=2, Å		3.20
CC(1/2) at which I/σI=1, %		17.2
CC(1/2) at which I/σI=2, %		44.1
Completeness (outer shell), %		99.7 (99.6)
R_{merge} (outer shell)%		20.6 (179.8)
No. of crystals used		1
No. of Reflections Used:	Observed	5,954,867
	Unique	1,181,400
Redundancy (outer shell)		5.04 (4.76)
Wilson B-factor, $Å^2$		104.3
Refinement		
R_{work}/R_{free}, %		23.8/29.2
No. of Non-Hydrogen Atoms		
RNA		199,951
Protein		90,976
Ions (Mg, K, Zn, Fe)		1,480
Waters		1,172
Ramachandran Plot		
Favored regions, %		93.71
Allowed regions, %		5.52
Outliers, %		0.77
Deviations from ideal values (RMSD)		
Bond, Å		0.003
Angle, degrees		0.650
Chirality		0.035
Planarity		0.004
Dihedral, degrees		15.222
Average B-factor (overall), $Å^2$		95.7

$R_{merge} = \Sigma |I - \langle I \rangle| / \Sigma I$, where I is the observed intensity and <I> is the average intensity from multiple measurements.
$R_{work} = \Sigma|F_{obs} - F_{calc}| / \Sigma F_{obs}$. For calculation of R_{free}, 5% of the truncated dataset was excluded from the refinement.

Table S3. Summary of possible base pairing interactions of pseudouridine in decoding. This table summarizes the possible base-pairing interactions between mRNAs and tRNAs that we observe in our reconstituted translation system. In *E. coli*, the $tRNA^{Val}$ anticodons are 5'-GAC and 5'-cmo^5UAC (29), which require the formation of a Ψ:C basepair during decoding of the ΨUU codon, as well as either a Ψ:G or Ψ:cmo^5U depending on which $tRNA^{Val}$ isoacceptor decodes the modified codon. The $tRNA^{Leu}$ anticodon sequences are 5'-CAG, 5'-GAG, 5'-$cmnm^5U_m$AA, 5'-C_mAA, and 5'-cmo^5UAA. These anticodons require Ψ to base pair with G or A to decode the ΨUU codon, and pairing with C, G, $cmnm^5U_m$, C_m, or cmo^5U when Ψ is in the third position. Anticodons $tRNA^{Ile}$ are 5'-GAU and 5'-k^2CAU, which both require a Ψ:U base pair in the first position. When present in tRNA anticodons, Ψ is known to base pair with A and G, and more broadly with A, G, and (in 16S rRNA).

Codon	Observed aa	Possible anticodons	Ψ base pair	Mismatch at other position
5'-ΨUU (1st pos)	valine	5'-GAC 5'-cmo^5UAC	Ψ:C	U:G (3rd pos) –
	leucine	5'-CAG 5'-GAG 5'-$cmnm^5U_m$AA 5'-C_mAA 5'-cmo^5UAA	Ψ:G Ψ:A	U:C (3rd pos) U:G (3rd pos) – – –
	isoleucine	5'-GAU 5'-k^2CAU	Ψ:U	U:G (3rd pos) U:k^2C (3rd pos)
5'-UUΨ (3rd pos)	valine	5'-GAC 5'-cmo^5UAC	Ψ:G Ψ:cmo^5U	C:U (1st pos) C:U (1st pos)
	leucine	5'-CAG 5'-GAG 5'-$cmnm^5U_m$AA 5'-C_mAA 5'-cmo^5UAA	Ψ:C Ψ:G Ψ: $cmnm^5U_m$ Ψ:C_m Ψ:cmo^5U	G:U (1st pos) G:U (1st pos) – – –

Table S4: Uridine-containing codons analyzed for elongation miscoding.

Amino acids evaluated for miscoding in 293H cells	Codons evaluated for miscoding in 293H cells
Phe	UUU, UUC
Leu	UUA, UUG, CUU, CUC, CUA, CUG
Ile	AUU, AUC, AUA
Val	GUU, GUC, GUA, GUG
Trp	UGG
Tyr	UAU, UAC

Table S5: This table summarizes the amino acid substitutions detected from U-containing Phe, Tyr, Leu codons in the KGPAPFYPLEDGTAGEQLHK peptide when mRNAs were synthesized with Ψ. The frequencies of the substitutions are also denoted. For calculating the frequencies, an extracted ion chromatogram was generated at <5ppm for each of the peptides of interest from the total ion current, and the area under the curve for each EIC was calculated. This was then used to calculate the percentage of substitution (area under the curve for peptides with a specific substitution/[area under the curve for all wild-type peptides with no substitution + area under the curve for all peptides with substitutions]).

	Substitutions observed	**Frequency of substitution (%)**
Phe	Ser, Ile/Leu	0.42
Tyr	Cys, His	0.19
Leu	Pro, Gln	0.52

Table S6: This table summarizes the amino acid substitutions detected in the U-containing codons in the entire luciferase dataset for multiple peptides when mRNAs were synthesized with Ψ. For calculating the frequencies, an extracted ion chromatogram was generated at <5ppm for each of the peptides of interest from the total ion current, and the area under the curve for each EIC was calculated. This was then used to calculate the percentage of substitution (area under the curve for peptides with a specific substitution/[area under the curve for all wild-type peptides with no substitution + area under the curve for all peptides with substitutions]).

	Substitutions observed	**Frequency of substitution (%)**
Phe	Ser, Ile, Glu	0.38
Tyr	His, Cys, Asp	0.11
Leu	Pro, Ser, Gln	0.47
Ile	Thr, Phe, Trp, Cys, Val	0.19
Val	Glu, Ala, Arg, Phe	0.2
Trp	Asp	0.142

Table S7. Observed rate constants for peptide release.

RF	codon	k_{max} (s^{-1})	95% CI
RF1	UAA	0.24[†]	(0.15 – 0.34)
	ΨAA	0.085[†]	(0.044 – 0.14)
	Um^6AA	0.23 ± 0.02[*]	–
	UAm^6A	0.19 ± 0.01[*]	–
RF2	UAA	0.061[†]	(0.029 – 0.11)
	ΨAA	0.077[†]	(0.050 – 0.11)
	Um^6AA	0.13 ± 0.02[*]	–
	UAm^6A	0.068 ± 0.003[*]	–

[†]Reported k_{max} values are the fitted maximum observed rate constants from the fits in Figure S3, along with the 95% confidence interval in the fitted value of k_{max}.
[*]Reported k_{max} values are the observed rate constants for reactions with 10 μM release factor. Error values are the standard error.

SUPPLEMENTARY FIGURES

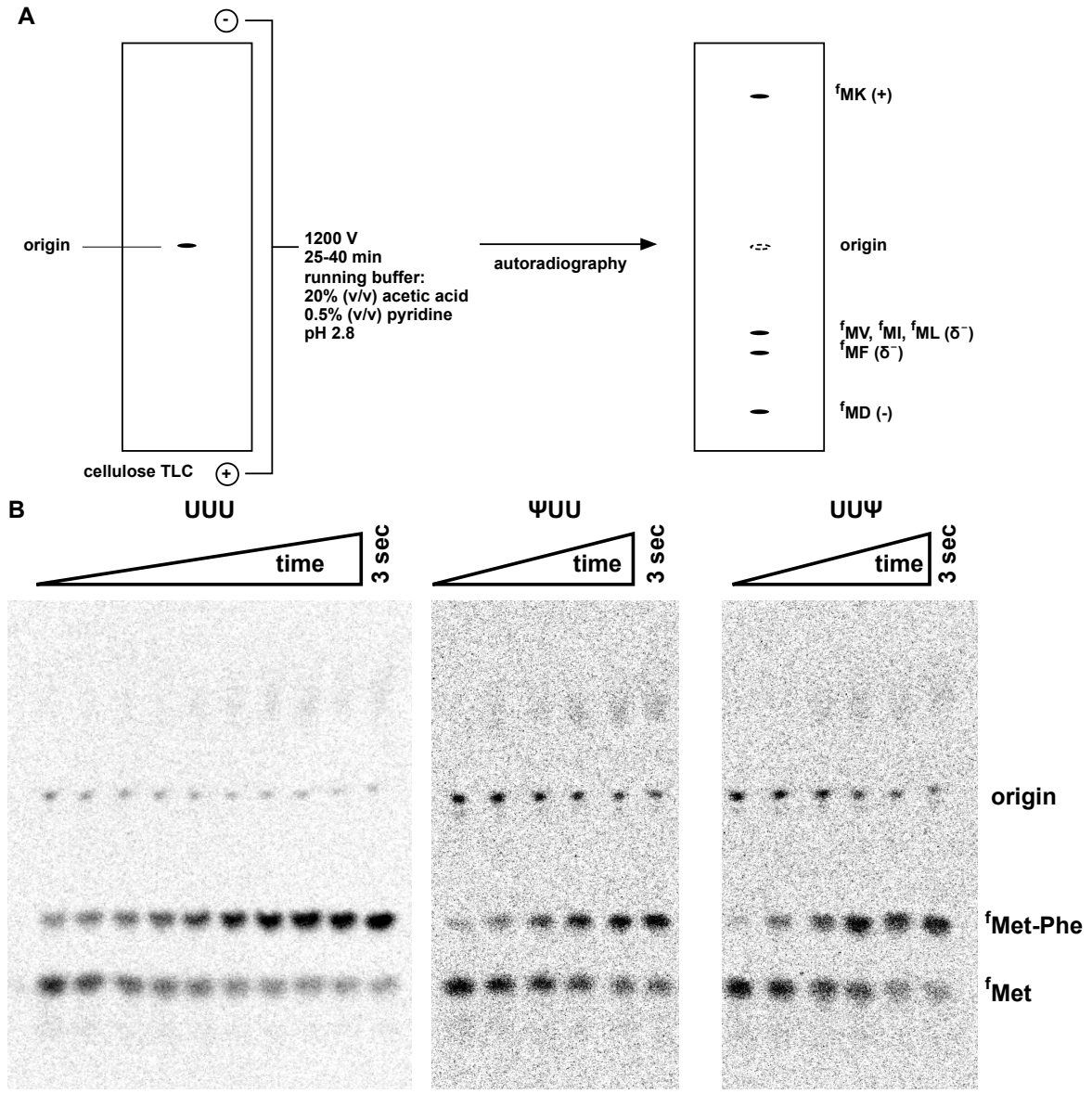

Figure S1. Electrophoretic TLC system used for separation and detection of peptide products. (A) Scheme showing how short, N-formyl-[^{35}S]- methionine-labeled peptides are separated by electrophoresis on a cellulose TLC in a volatile, acidic buffer, and detected by phosphorimaging. Peptide migration is determined primarily by the net charge and secondarily by the identity of the amino acid R groups. **(B)** Representative images of time courses for the data in Figure 2 are shown. The brightness and contrast of these images have been adjusted to clearly show all bands and the background, and as a consequence pixel intensity is no longer linear with signal.

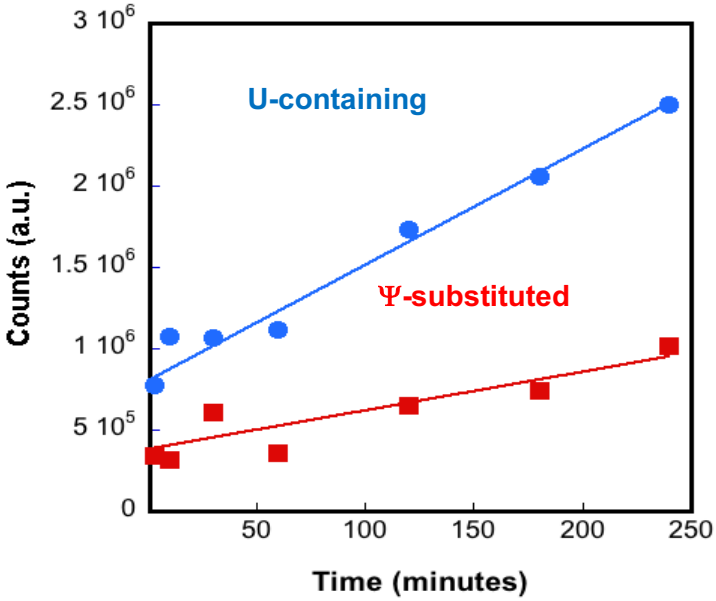

Figure S2. Fully substituted pseudouridinylated mRNA produces less full-length protein in a bacterial in vitro translation system. Luciferase mRNA was in vitro transcribed in the presence of either uridine triphosphate or pseudouridine triphosphate, and in vitro translated using the NEB PURExpress® system in the presence of L-[^{35}S]-methionine. Protein products were separated by SDS-PAGE and the full-length luciferase protein was quantified by phosphorimaging. The y-axis is the integrated photostimulated luminescence units in the full-length luciferase band and the x-axis is the reaction time. The experiment was performed twice; a representative plot is shown.

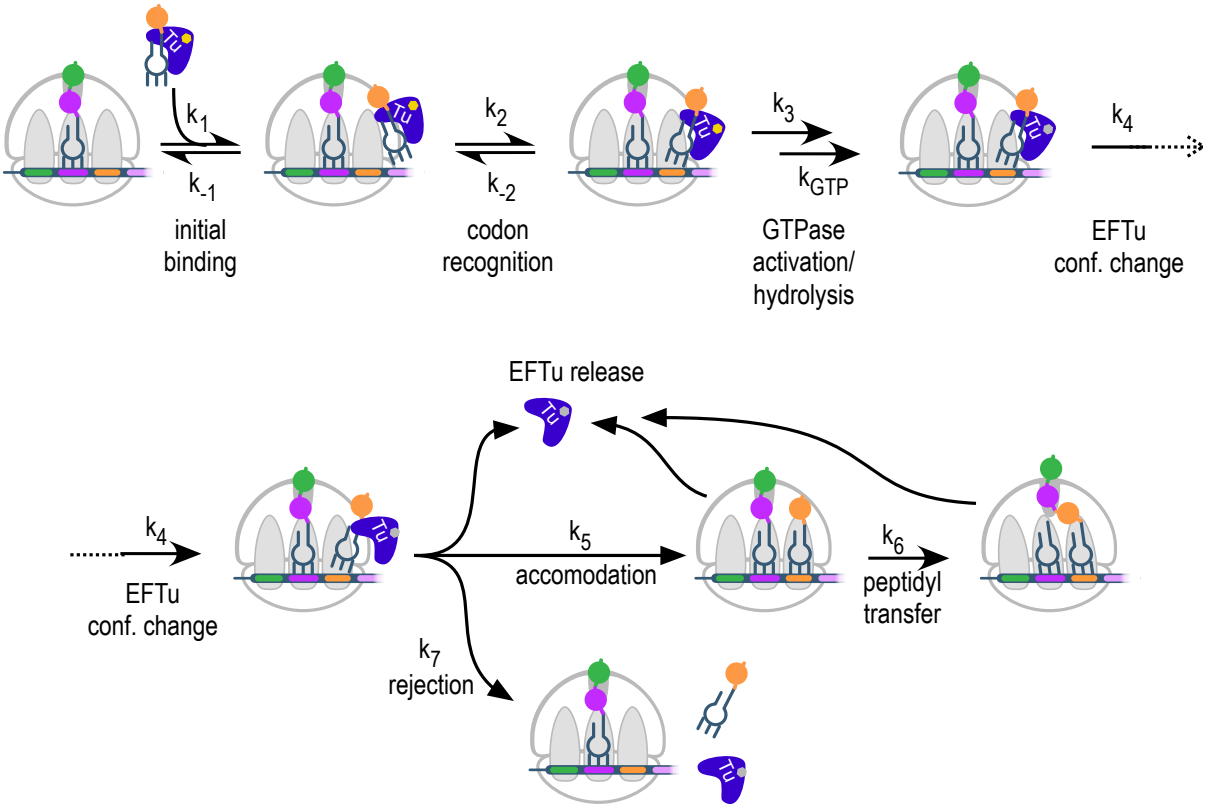

Figure S3. Mechanistic model for tRNA selection and amino acid addition. The observed rate constants from experiments in Figure 1 are a function of all shown rate constants. The observed rate constants for GTP hydrolysis in Figure 2 reflect the rate constants for initial binding through GTPase activation and hydrolysis. The model shown is based on published models from Rodnina and coworkers (30, 31).

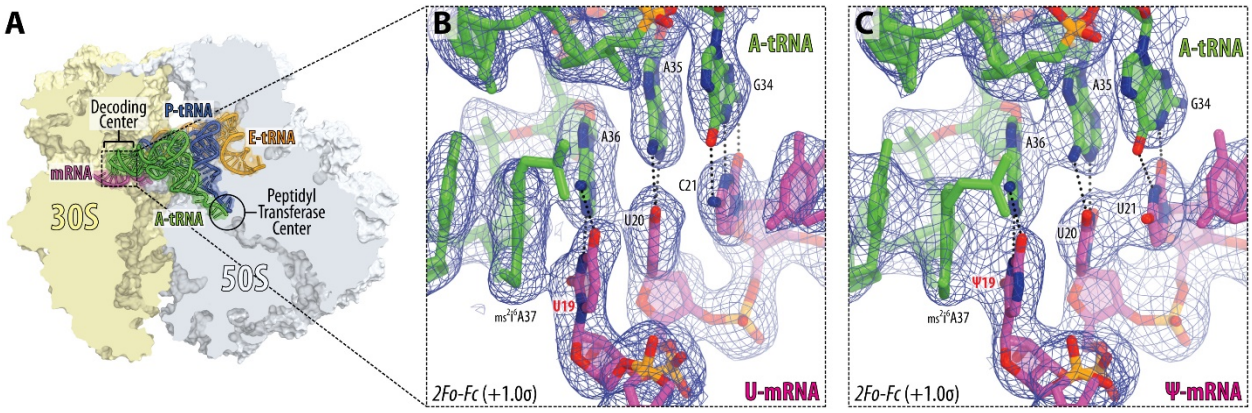

Figure S4. The electron density maps showing codon-anticodon interactions of tRNA^{Phe} with regular *vs.* Ψ-containing mRNA. (A) Overview of the 70S ribosome from *T. thermophilus* showing locations of main ribosomal functional centers: the decoding center and the peptidyl transferase center. The view is from the cytoplasm onto the A site. 30S subunit is shown in light yellow, 50S subunit is in light blue. mRNA is shown in magenta and tRNAs are displayed in green for the A site, in dark blue for the P site, and in orange for the E site. **(B, C)** Close-up views of the *2Fo-Fc* electron difference Fourier maps (blue mesh) around the decoding center showing codon-anticodon interactions of tRNA^{Phe} with either unmodified mRNA **(C)** or Ψ-containing mRNA **(D)**. In **(C)**, both the map and the model are from PDB entry 4Y4P (8). H-bond interactions of the mRNA codon (nucleotides 19-21) with the tRNA anticodon (nucleotides 34-35) are indicated with the dashed black lines. The refined models of mRNA (magenta) and tRNA (green) are displayed in their respective electron densities contoured at 1.0σ. Nitrogen atoms of codon and anticodon nucleotides are colored blue; oxygens are red. Note that no major differences could be observed between the 70S complexes bound to regular mRNA *vs.* Ψ-containing mRNA.

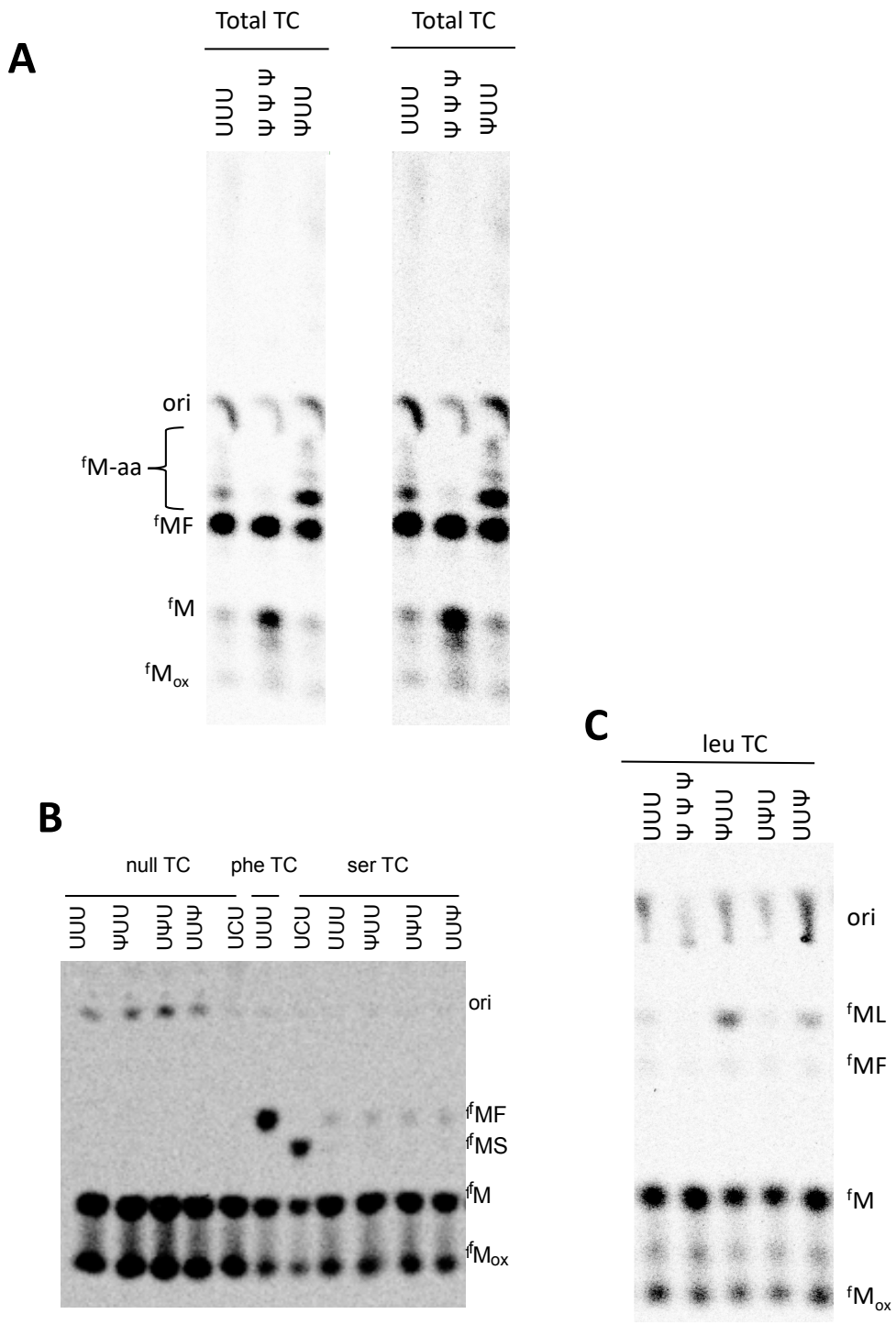

Figure S5. Increased amino acid substitution on Ψ-containing UUU codons, relative to unmodified UUU codons in vitro. (A) Electrophoretic TLC displayed at low (left) and high (right) contrast showing the translation products of UUU, ΨΨΨ, and ΨUU-containing messages in the reacted with the same TC containing total aa-tRNA. Total tRNA was aminoacylated with a mixture of all possible 20 amino acids using S100 extract, as described in our methods. A higher level of

amino acid substitution is observed on the modified ΨUU codon relative to the UUU codon. **(B)** Serine does not incorporate on Ψ-containing phenylalaine codons in vitro. Electrophoretic TLC displaying the translation products of UCU (serine codon), unmodified and Ψ-containing messages in the presence of no tRNA (null), Phe-tRNA^{Phe} tRNA (phe TC), total tRNA aminoacylated with serine (ser TC). **(C)** Leucine substitution of enhanced on Ψ-containing phenylalaine codons in vitro. Electrophoretic TLC displaying the translation products of UUU and Ψ-substituted codons (ΨΨΨ, ΨUU, UΨU, UUΨ) the presence of TCs formed with total tRNA aminoacylated with leucine (leu TC). More leucine is incorporated on ΨUU and UUΨ codons relative to UUU.

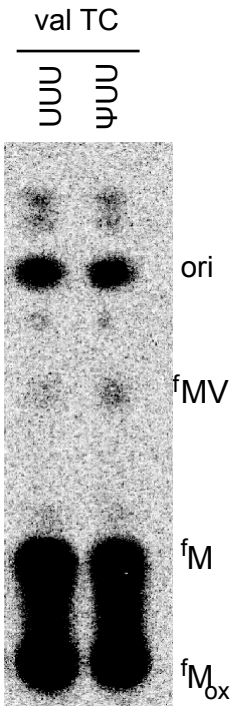

Figure S6. Alternative decoding by pseudouridine-containing codons depends on the sequence context of the modified codon. Initiation complexes were formed on mRNAs containing a UUU or ΨUU codon as the second codon in an mRNA coding for MFKKX and reacted with Val-tRNAVal ternary complex. Electrophoretic TLC displaying the translation products of unmodified and 1st position Ψ-containing messages in the presence of total tRNA aminoacylated with valine (val TC).

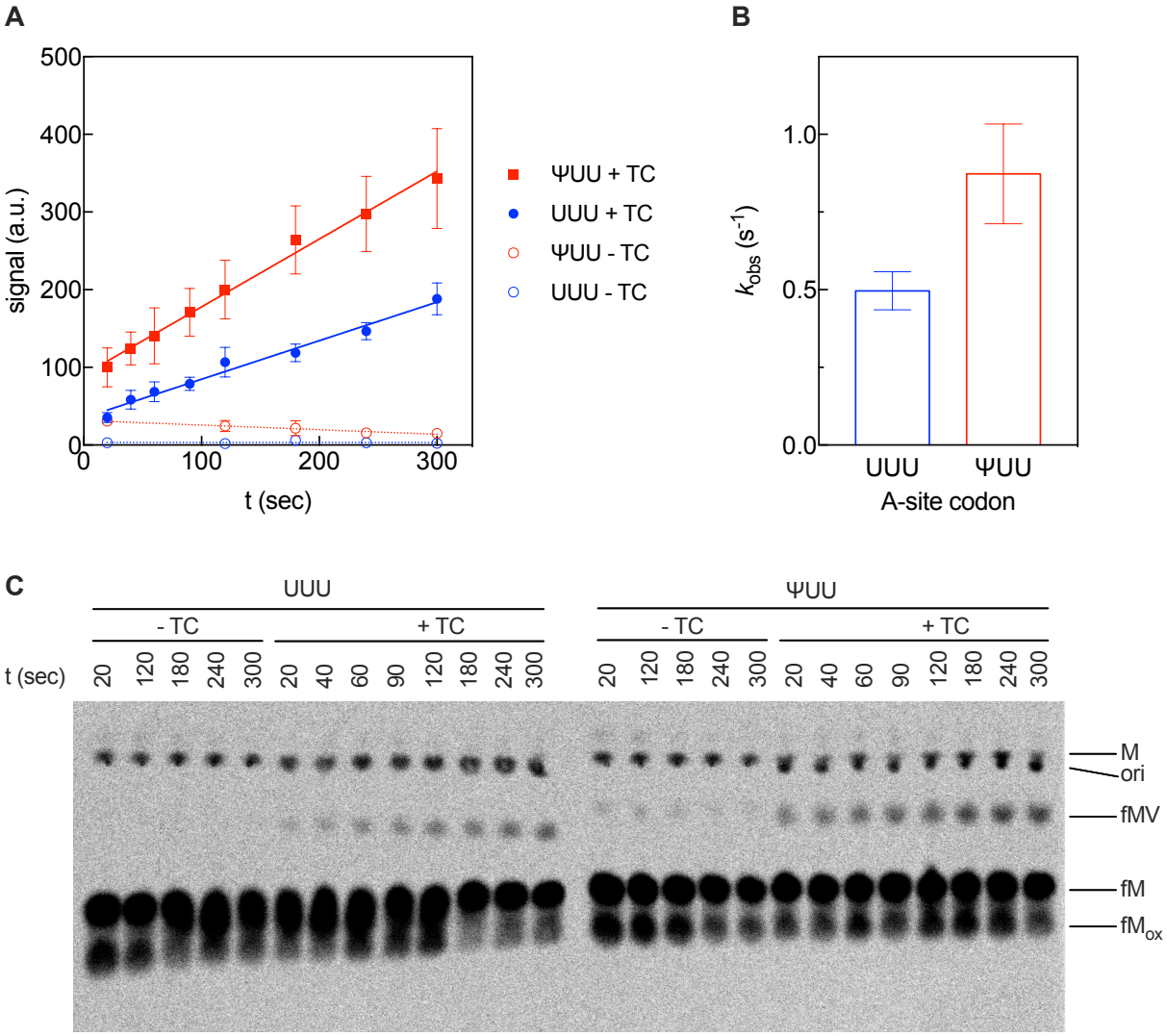

Figure S7. Valine is incorporated more rapidly on a ΨUU codon than on a UUU codon. Excess Val-$tRNA^{Val}$ (10 μM) was reacted with 100 nM initiation complexes in the presence of 40 μM EFTu, 10 mM free Mg^{2+}, GTP, and an energy regeneration system. **(A)** Signal (integrated photostimulated luminescence units) in the ^{f}Met-Valine band is plotted as a function of time for initiation complexes reacted with the ternary complex (+), or buffer only (-). Each point is the mean from three independent experiments and the error bars are the standard error of the mean. **(B)** Observed rate constants for the linear fits of + ternary complex reactions in A. Error bars are the 95% confidence intervals on the fitted value of k_{obs}. **(C)** One of the three electrophoretic TLCs used to generate the data in **(A)** and **(B).**

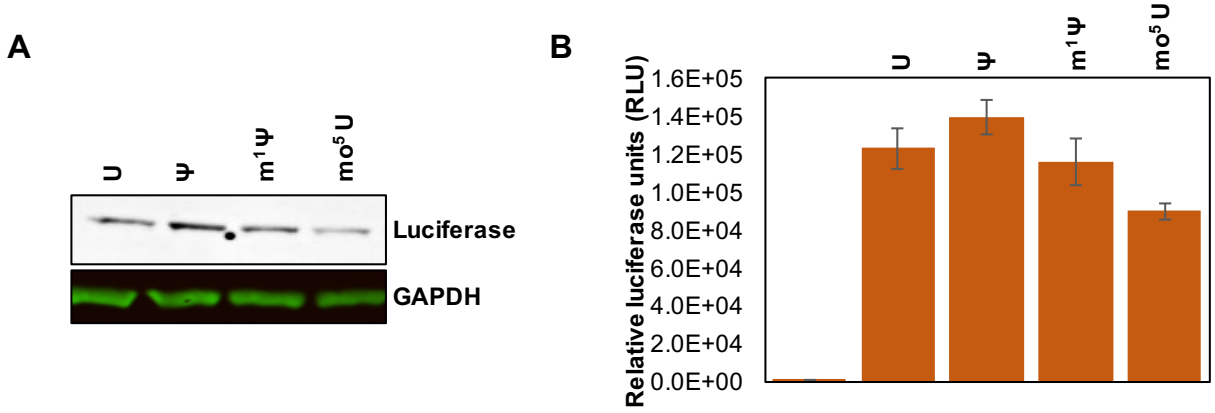

Figure S8. Expression of luciferase mRNA *in vivo*. (A) Western blot analysis of the full-length luciferase products purified from 293H cells after expression of luciferase mRNA synthesized with either standard (U) or modified (Ψ, $m^1Ψ$, mo^5U) nucleotides. $m^1Ψ$ and mo^5U were used as a control to check the effect of other uridine analogs on the expression of the luciferase mRNA. **(B)** Luciferase activity assay demonstrating functionality of unmodified and modified luciferase mRNAs.

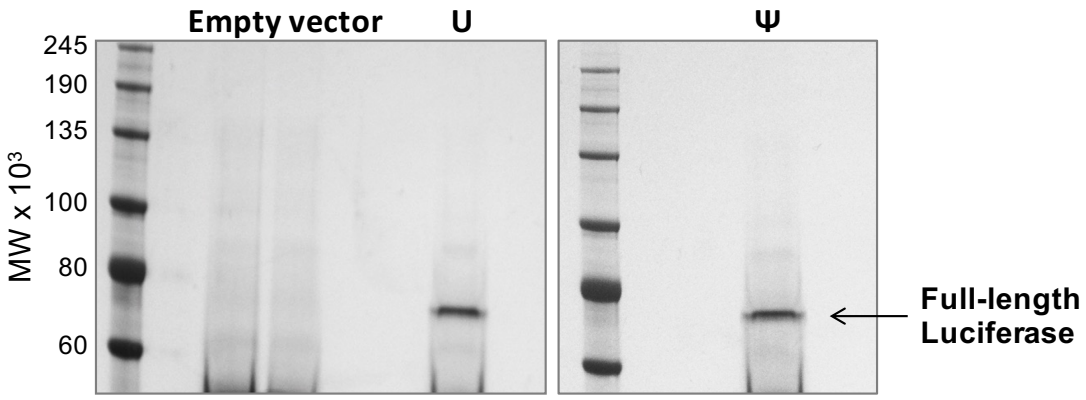

Figure S9: Silver-stained SDS/PAGE gel showing the purification of luciferase protein from 293H cells when transfected with either U-containing or Ψ-containing luciferase mRNAs.

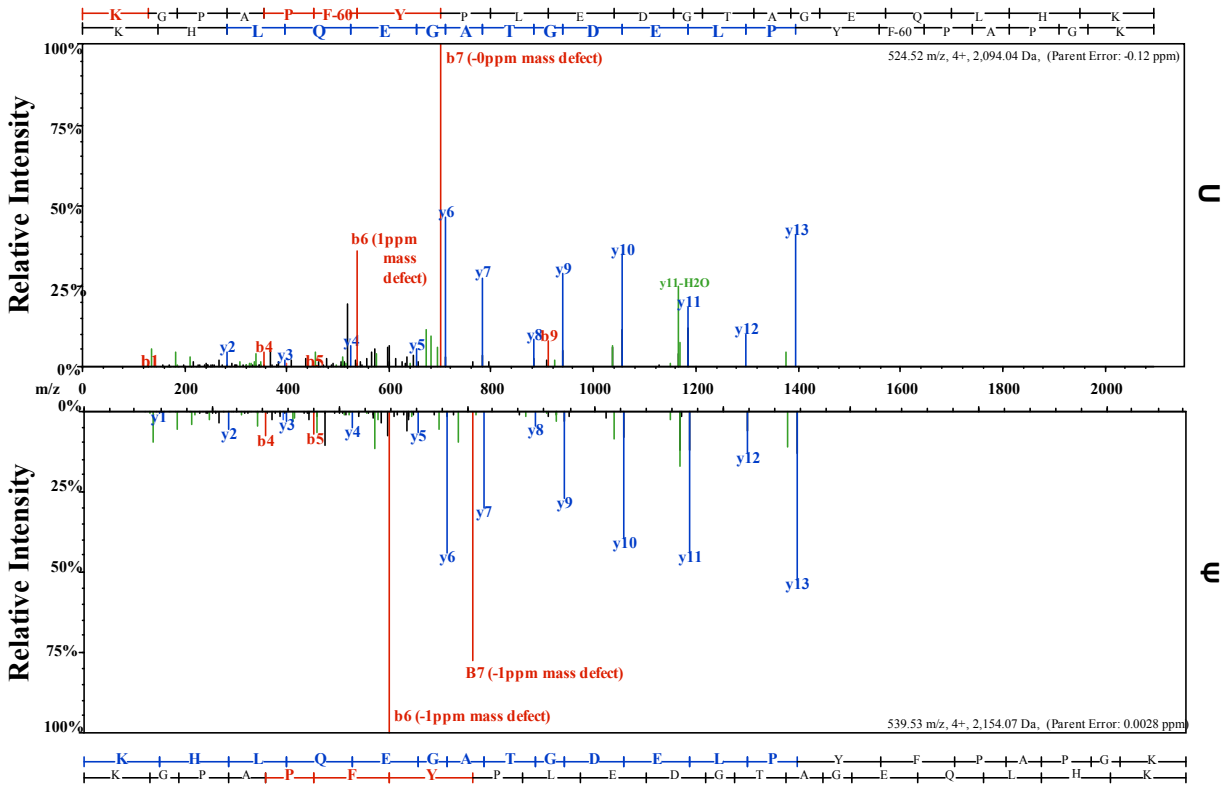

Figure S10. Fragmentation spectra showing Phe to Ser substitution in peptides from Ψ-containing mRNA. Results from the error-tolerant search were loaded onto Scaffold (Proteome Software, version 4.8.7) and DDA fragmentation spectra from a proteotypic peptide were compared. The site of modification (Phe46) was covered by two adjacent fragment ions in both peptides, b6 and b7, with all relevant precursor and fragment ions identified with < 2ppm mass accuracy. The peptide generated from the unmodified U-containing mRNA has an m/z for phenylalanine at position 46 (bottom panel). In contrast, the peptide generated from Ψ-containing mRNA demonstrates an m/z for serine, not phenylalanine at position 46 (top panel). The nominal mass difference between serine and phenylalanine is 60 Da, and the serine is denoted as F-60 in the top panel.

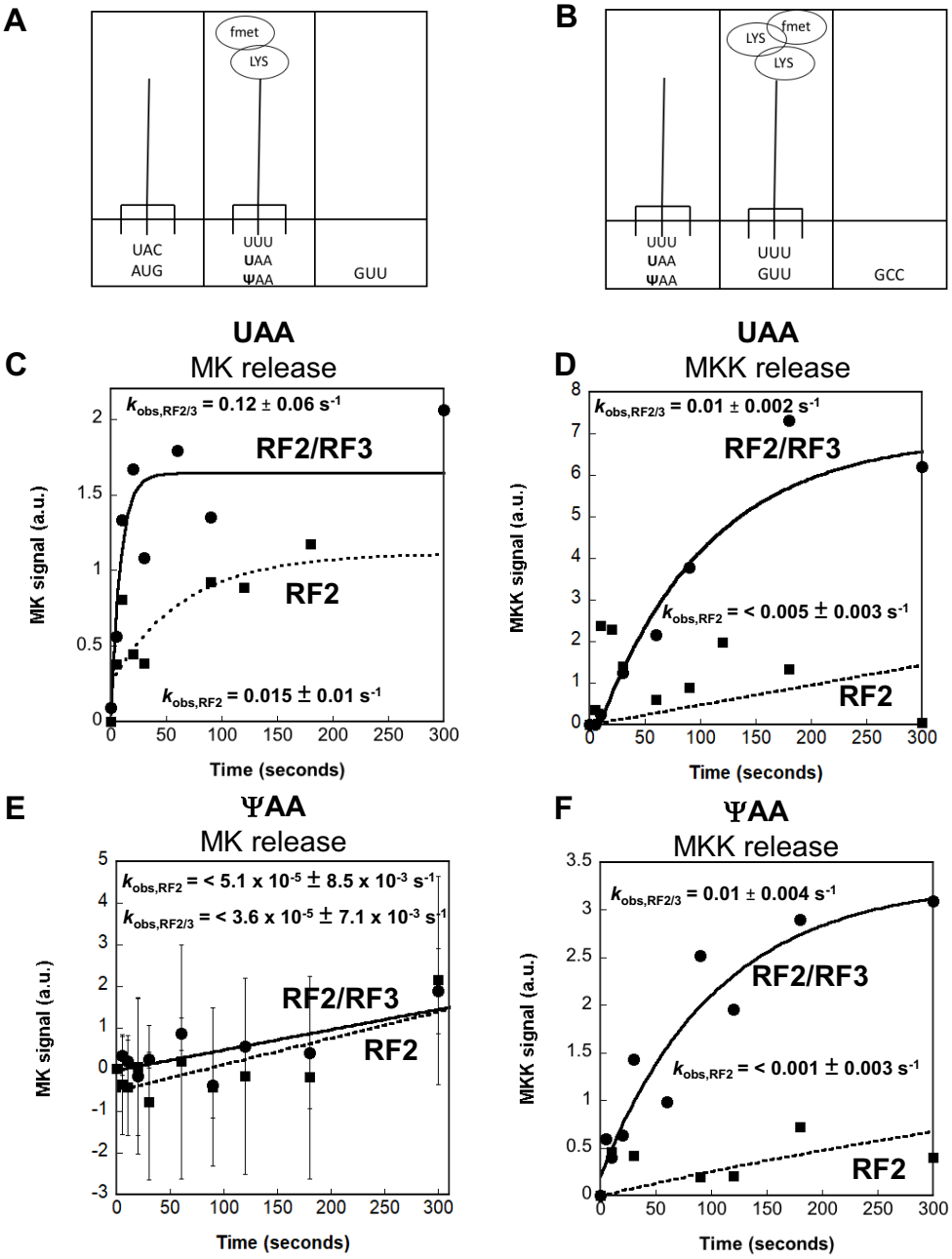

Figure S11. P site mismatch surveillance mechanism is not triggered by amino acid substitution on Ψ-containing codon. Panels A and B summarize the position of the codons and peptidyl-tRNA and codons in the purified ribosome elongation complexes prior to addition of RF2 and RF2/RF3. **(A)** Codons in the E-, P- and A site (left to right) when the MK peptide is attached to the mismatched tRNA in the P site. **(B)** Codons in the E-, P- and A site (left to right) when the MKK peptide is attached to the mismatched tRNA in the P site. While a de-acylated tRNA is displayed for clarity in the E site of A and B, in all likelihood, has dissociated from the ribosome in our complexes. Panels C and D are example experiments in which MK **(C)** and MKK **(D)** peptide release is catalyzed by RF2 and RF2/RF3 from an unmodified mRNA. As expected, because there is a mismatch between the tRNA anticodon and mRNA codon in the P site, MK and MKK are released in an RF2-dependent manner from the ribosome. In both cases, the rate constant for peptide release is enhanced by at least 10-fold when RF3 is present. Panels C and D are

example experiments on a Ψ-modified mRNA. In these assays, RF2 or RF2/RF3 are added to complexes with either MK-tRNA^{Lys} **(C)** or MKK-tRNA^{Lys} **(D)** bound to a mis-matched codon in the P site (as shown in panels A and B). Notably, MK release was not catalyzed in five separate experiments when ΨAA is in the P site; each of the time courses we collected generated scatter plots. The points displayed on the plot in panel E are the average of points from three identical time-courses, and the error bars reflect the range in values measured. In contrast to MK release on the UAA message, these plots could not be meaningfully fit (see errors on fits) and RF3 did not enhance the rate constant for MK release, as happens when the P site surveillance mechanism is triggered. This suggests that the ribosome does not read the tRNA^{Lys}:mRNA pairing as a mismatch on the ΨAA codon in the P site. However, as shown in panel **F**, when a mismatch occurs on the same message between tRNA^{Lys} and a GUU codon (see Fig. S11B), the P site surveillance mechanism is activated and MKK is released in an RF2/RF3 dependent manner. As on the unmodified message, the rate constant for MKK release is significantly enhanced by the presence of RF3. These experiments were repeated on at least 4 different days, and all experimental repeats consistently demonstrated the RF2/RF3 dependent release of both MK and MKK from the unmodified message, and only MKK from the modified message.

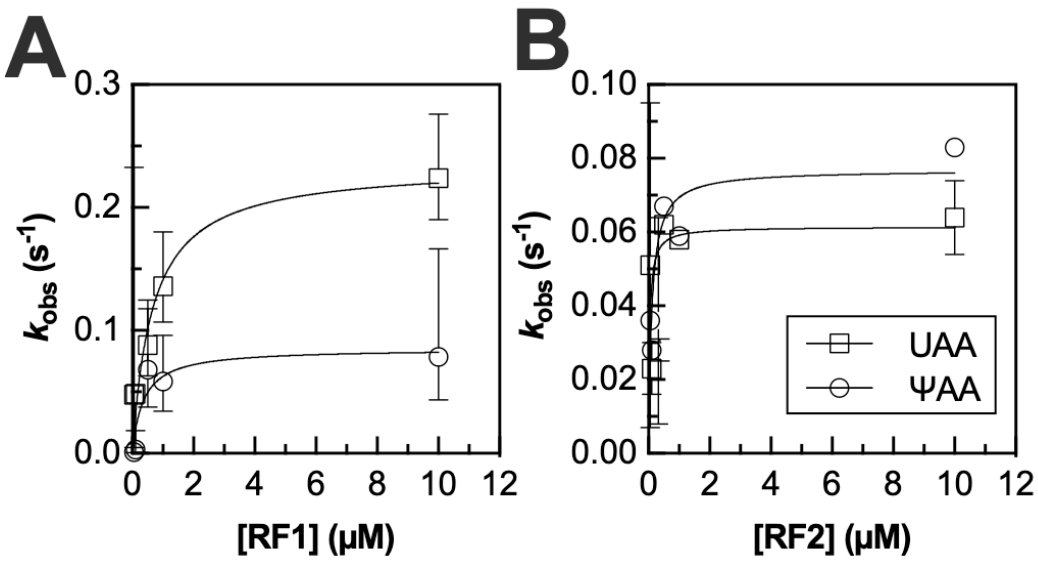

Figure S12. Peptide release on the ΨAA codon is slightly perturbed
k_{obs} values were measured at range of RF1 **(A)** and RF2 **(B)** concentrations. Each time course was repeated at least twice and error bars are the standard error of the fitted value of k_{obs}.

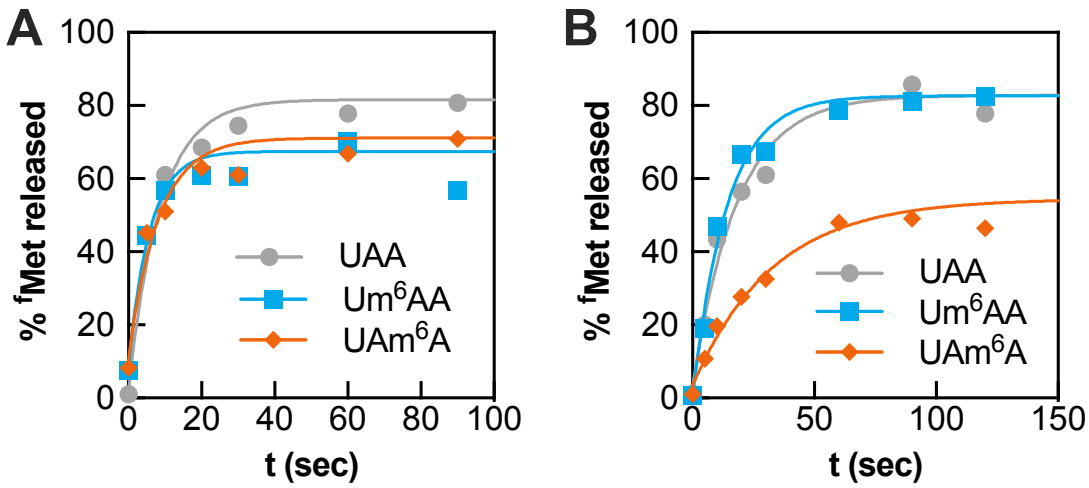

Figure S13. Endpoint defects on m^{6}A-containing stop codons are rescued by additional RF2. Several chemical modifications in stop codons alter the activity of release factors (28), but m^{6}A has not been investigated. We measured the rate constants for ^{f}Met release on mRNAs containing m^{6}A modifications to the universal stop codon (Um^{6}AA/UAm^{6}A). We found that m^{6}A did not change the rate constants for peptide release by either RF1 **(A)** or RF2 **(B)** (Table S7), but did reduce the yield for release catalyzed by 1 μM RF2 on a UAm^{6}A modified codon (82% for UAA, and 55% for UAm^{6}A). This end-point defect was rescued by the addition of 10 μM RF2 (92% for UAA, 90% for Um^{6}AA) (Fig. S14).

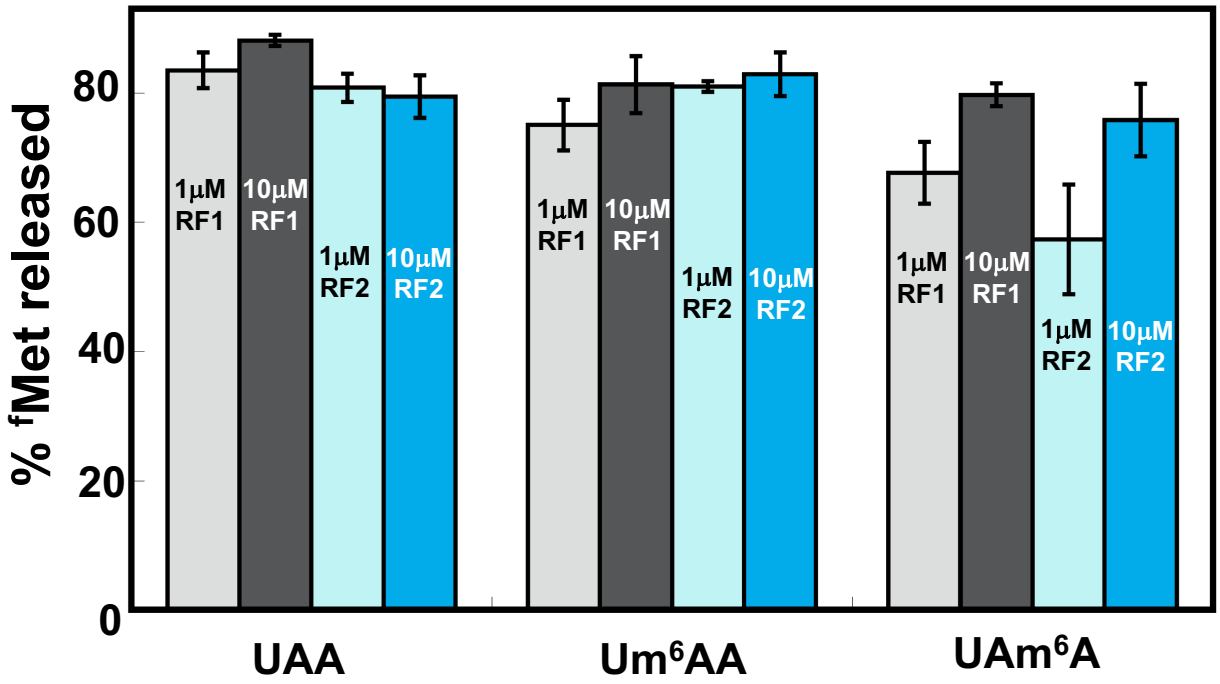

Figure S14. Endpoint defect on UAm^{6}A-containing stop codon is rescued by additional RF2.

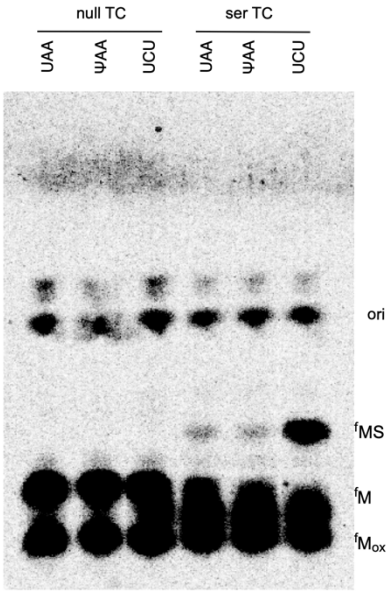

Figure S15. A ΨAA-modified stop codon does not enhance serine incorporation in vitro. Electrophoretic TLC displaying the translation products of unmodified and Ψ-containing stop codon messages in the presence of no tRNA (null), total tRNA aminoacylated with serine (ser TC).

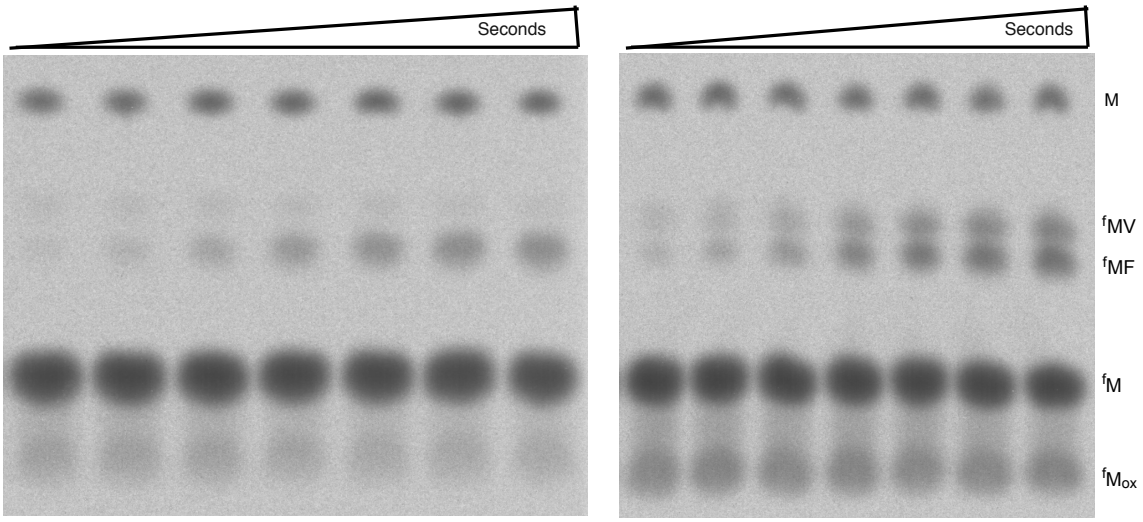

Figure S16. Magnesium dependence of competition between Val-tRNAVal ternary complex Phe-tRNAPhe ternary complex on a ΨUU codon. ΨUU initiation complexes (100 nM) were reacted with 50 nM Phe-tRNA^{Phe} and 20 μM Val-tRNA^{Val} in the presence of 10 nM EFTu, EFTs, energy regeneration mix, and low (sub-mM) or high (~ 10 mM) free Mg(II). Almost no fMet-Val dipeptide is formed at low magnesium concentrations, while at high magnesium concentrations fMet-Val formation is almost stoichiometric with fMet-Phe.

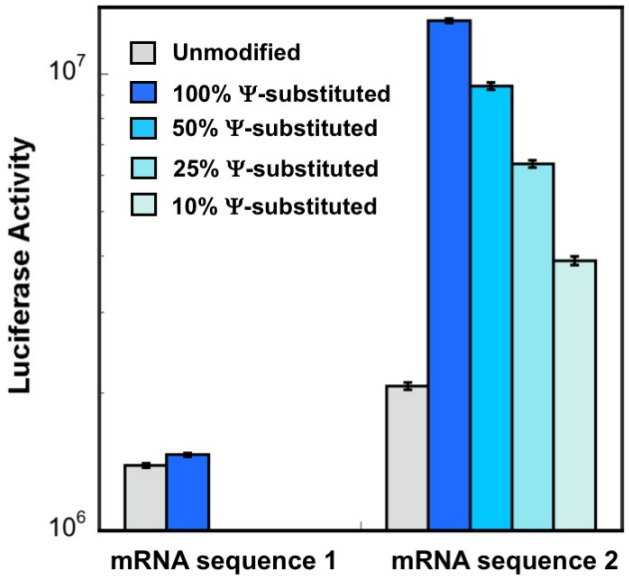

Figure S17. The yield of active protein from pseudouridinylated mRNAs depends on the level of pseudouridinylation and sequence context. Two mRNAs coding for luciferase but with silent coding region changes were in vitro transcribed in the presence of varying ratios of uridine and pseudouridine triphosphate. Purified mRNAs were transfected into cultured mammalian cells and luciferase activity was assayed at a single time point.

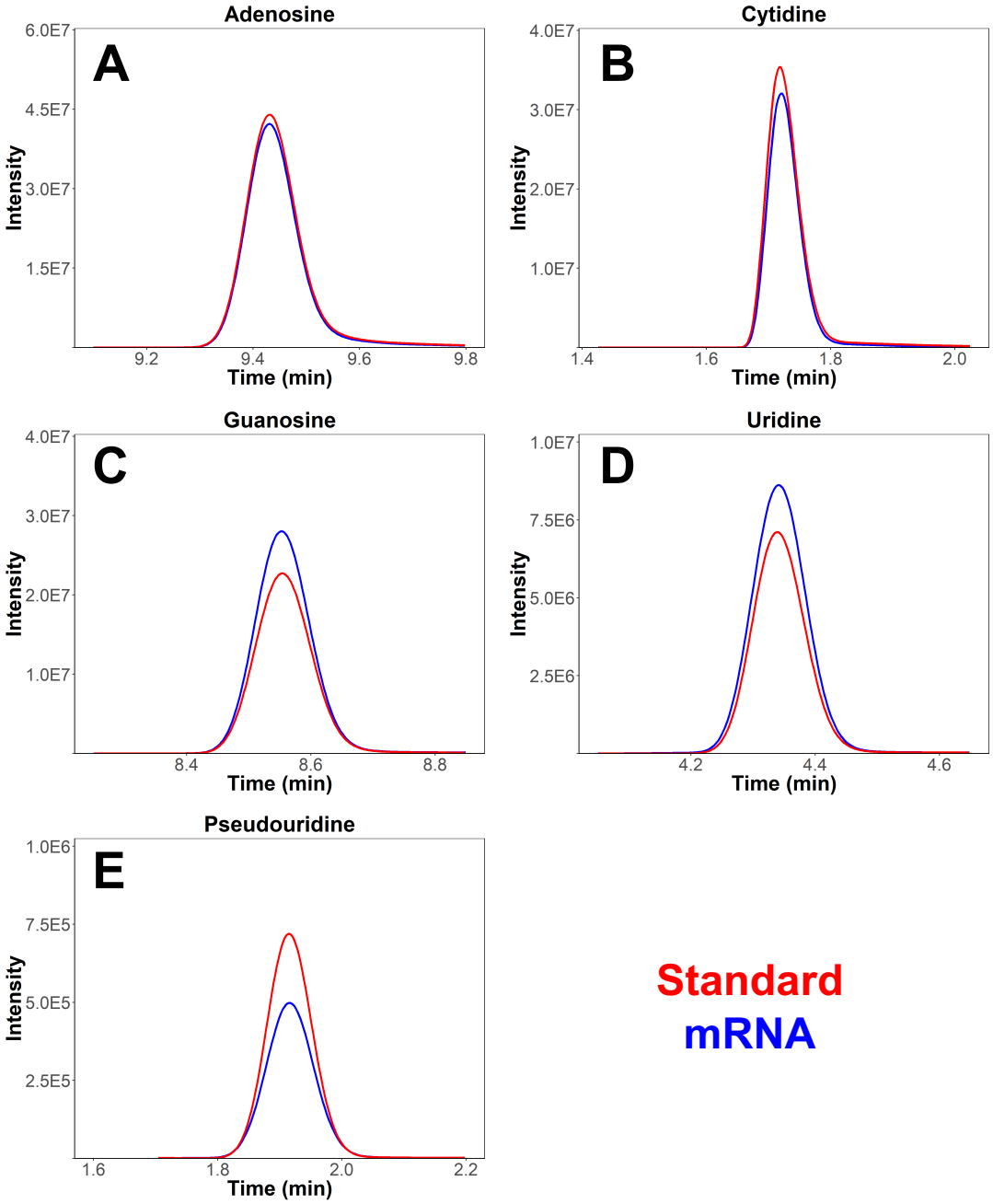

Figure S18. Verification of pseudouridine in synthetic mRNAs. Overlaid extracted ion chromatograms of the four main bases **(A-D)** and pseudouridine **(E)** in a nucleoside standard (red line) and synthetic mRNA oligonucleotide (blue line). Note that the ranges on the x-axes vary from panel to panel.

References for SI Appendix

1. Milligan JF, Groebe DR, Witherell GW, & Uhlenbeck OC (1987) Oligoribonucleotide synthesis using T7 RNA polymerase and synthetic DNA templates. *Nucleic Acids Res* 15(21):8783-8798.
2. Walker SE & Fredrick K (2008) Preparation and evaluation of acylated tRNAs. *Methods* 44(2):81-86.
3. Basanta-Sanchez M, Temple S, Ansari SA, D'Amico A, & Agris PF (2016) Attomole quantification and global profile of RNA modifications: Epitranscriptome of human neural stem cells. *Nucleic Acids Res* 44(3):e26.
4. Pavlov MY*, et al.* (1998) A direct estimation of the context effect on the efficiency of termination. *J Mol Biol* 284(3):579-590.
5. Maracci C, Peske F, Dannies E, Pohl C, & Rodnina MV (2014) Ribosome-induced tuning of GTP hydrolysis by a translational GTPase. *Proc Natl Acad Sci U S A* 111(40):14418-14423.
6. Zaher HS & Green R (2009) Quality control by the ribosome following peptide bond formation. *Nature* 457(7226):161-166.
7. Koutmou KS*, et al.* (2015) Ribosomes slide on lysine-encoding homopolymeric A stretches. *Elife* 4.
8. Polikanov YS, Melnikov SV, Soll D, & Steitz TA (2015) Structural insights into the role of rRNA modifications in protein synthesis and ribosome assembly. *Nat. Struct. Mol. Biol.* 22(4):342-344.
9. Selmer M*, et al.* (2006) Structure of the 70S ribosome complexed with mRNA and tRNA. *Science* 313(5795):1935-1942.
10. Korostelev A, Trakhanov S, Laurberg M, & Noller HF (2006) Crystal structure of a 70S ribosome-tRNA complex reveals functional interactions and rearrangements. *Cell* 126(6):1065-1077.
11. Polikanov YS, Blaha GM, & Steitz TA (2012) How hibernation factors RMF, HPF, and YfiA turn off protein synthesis. *Science* 336(6083):915-918.
12. Kabsch W (2010) Xds. *Acta Crystallogr. D. Biol. Crystallogr.* 66(Pt 2):125-132.
13. McCoy AJ*, et al.* (2007) Phaser crystallographic software. *J. Appl. Crystallogr.* 40(Pt 4):658-674.
14. Adams PD*, et al.* (2010) PHENIX: a comprehensive Python-based system for macromolecular structure solution. *Acta Crystallogr. D Biol. Crystallogr.* 66(Pt 2):213-221.
15. Emsley P & Cowtan K (2004) Coot: model-building tools for molecular graphics. *Acta Crystallogr. D Biol. Crystallogr.* 60:2126-2132.
16. Roy B, Leszyk JD, Mangus DA, & Jacobson A (2015) Nonsense suppression by near-cognate tRNAs employs alternative base pairing at codon positions 1 and 3. *Proc Natl Acad Sci U S A* 112(10):3038-3043.
17. Roy B*, et al.* (2016) Ataluren stimulates ribosomal selection of near-cognate tRNAs to promote nonsense suppression. *Proc Natl Acad Sci U S A* 113(44):12508-12513.
18. Fernandez IS*, et al.* (2013) Unusual base pairing during the decoding of a stop codon by the ribosome. *Nature* 500(7460):107-110.
19. Karijolich J & Yu YT (2011) Converting nonsense codons into sense codons by targeted pseudouridylation. *Nature* 474(7351):395-398.
20. Parisien M, Yi C, & Pan T (2012) Rationalization and prediction of selective decoding of pseudouridine-modified nonsense and sense codons. *RNA* 18(3):355-367.

21. Svidritskiy E, Madireddy R, & Korostelev AA (2016) Structural Basis for Translation Termination on a Pseudouridylated Stop Codon. *J Mol Biol* 428(10 Pt B):2228-2236.
22. Mora L, Heurgue-Hamard V, de Zamaroczy M, Kervestin S, & Buckingham RH (2007) Methylation of bacterial release factors RF1 and RF2 is required for normal translation termination in vivo. *J Biol Chem* 282(49):35638-35645.
23. Youngman EM, Brunelle JL, Kochaniak AB, & Green R (2004) The active site of the ribosome is composed of two layers of conserved nucleotides with distinct roles in peptide bond formation and peptide release. *Cell* 117(5):589-599.
24. Zavialov AV, Mora L, Buckingham RH, & Ehrenberg M (2002) Release of peptide promoted by the GGQ motif of class 1 release factors regulates the GTPase activity of RF3. *Mol Cell* 10(4):789-798.
25. Hetrick B, Lee K, & Joseph S (2009) Kinetics of stop codon recognition by release factor 1. *Biochemistry* 48(47):11178-11184.
26. Kuhlenkoetter S, Wintermeyer W, & Rodnina MV (2011) Different substrate-dependent transition states in the active site of the ribosome. *Nature* 476(7360):351-354.
27. Burakovsky DE*, et al.* (2010) Mutations at the accommodation gate of the ribosome impair RF2-dependent translation termination. *RNA* 16(9):1848-1853.
28. Hoernes TP*, et al.* (2018) Atomic mutagenesis of stop codon nucleotides reveals the chemical prerequisites for release factor-mediated peptide release. *Proc Natl Acad Sci U S A* 115(3):E382-E389.
29. Boccaletto P*, et al.* (2018) MODOMICS: a database of RNA modification pathways. 2017 update. *Nucleic Acids Res* 46(D1):D303-D307.
30. Pape T, Wintermeyer W, & Rodnina MV (1998) Complete kinetic mechanism of elongation factor Tu-dependent binding of aminoacyl-tRNA to the A site of the E. coli ribosome. *EMBO J* 17(24):7490-7497.
31. Ranjan N & Rodnina MV (2017) Thio-Modification of tRNA at the Wobble Position as Regulator of the Kinetics of Decoding and Translocation on the Ribosome. *J Am Chem Soc* 139(16):5857-5864.